

# THE USE OF $^2\text{H}$ AND $^{18}\text{O}$ ISOTOPES IN THE STUDY OF COASTAL KARSTIC AQUIFER

Diana Mance<sup>1</sup>, Danijela Lenac<sup>2</sup>, Maja Radišić<sup>3</sup>, Davor Mance<sup>4</sup>, Josip Rubinić<sup>3</sup>

<sup>1</sup>University of Rijeka, Faculty of Physics, Radmile Matejčić 2 – 51000 Rijeka (Croatia),  
phone: +385 51 5847811, e-mail: [diana.mance@uniri.hr](mailto:diana.mance@uniri.hr)

<sup>2</sup>Water Supply Company, Rijeka (Croatia)

<sup>3</sup>University of Rijeka, Faculty of Civil Engineering, Rijeka (Croatia)

<sup>4</sup>University of Rijeka, Faculty of Economics, Rijeka (Croatia)

**Abstract** – Karst covers nearly half of Croatia's area. Croatian karst is part of the Dinaric karst and stretches from the Adriatic Sea to the Pannonian basin. Carbonate aquifers are the primary source of freshwater in karst part of Croatia and their protection is of the highest priority. Karst aquifers are sensitive to pollution since pollutants can easily enter the groundwater channel systems, often without prior self-purification process. Once pollutants enter the karstic underground they spread through the aquifer very quickly. Therefore, a thorough knowledge of the karst aquifer is essential for a timely and appropriate reaction to possible pollution incidents. Complexity of the karst landforms and groundwater networks requires implementation of a standard hydrogeological monitoring as well as unconventional methods of investigation.

Analysis of stable water isotopes  $^2\text{H}$  and  $^{18}\text{O}$  proved to be helpful complementing method to a standard hydrogeological karst studies. We present the results of the stable isotope composition analysis of the coastal karst springs in the Bakar Bay and rain water collected in the hinterland of the springs. The local water supply company supervises the examined springs. During two years, spring water samples were collected on a weekly basis and rain samples were collected once a month.

The stable isotope composition of the karst groundwater was modelled using autoregressive integrated moving average modelling. The study's main findings are: winter precipitation of Mediterranean origin dominates springs recharge, a dual porosity model that includes a fissure-porous aquifer and karstic channels is a fit for the studied systems, and autocorrelation function analysis revealed varying degrees of karstification in the hinterland of the studied springs.

## Introduction

Karst aquifers are important sources of potable water not only in the Mediterranean region, but also globally [18]. They are recognized by their heterogeneous physical properties and complex flow patterns, which make investigation and description of their functioning challenging [5,14]. Many physicochemical parameters of groundwater could be used to characterize the hydrological behaviour of karst watersheds. However, in the case of non-stationary hydrological conditions, hydrochemical data should be supplemented with additional data such as environmental isotopes (e.g. water isotopes  $^{18}\text{O}$  and  $^2\text{H}$ ) to provide a reliable interpretation of karst basin functioning [15]. Some applications of water stable

isotopes in karst aquifer research include the analysis of recharge processes [8,13] and water reservoir mixing [12], as well as the determination of residence times [19] and mean recharge elevations [16].

Although stable isotopes are typically used to supplement traditional hydrological methods [6], it has been demonstrated that when conventional parameters are unavailable, a thorough statistical analysis of oxygen and hydrogen stable isotope time series could be used for description of karst system hydrological behaviour [7]. Stable isotope content of Bakar Bay springs (Perilo - PER, Dobra - DB, and Dobrica - DBC) are discussed in the paper. Since there is no data on discharges for these springs, in our analysis we had to rely entirely on stable isotopes and statistical modelling.

## Materials and Methods

An element's isotopes share the same number of protons but differ in the number of neutrons in their atomic nuclei. There are two stable isotopes of hydrogen:  $^1\text{H}$  and  $^2\text{H}$ . The lighter hydrogen isotope accounts for  $\approx 99.985\%$  of total stable hydrogen, with the heavier isotope  $^2\text{H}$  accounting for the remaining  $\approx 0.015\%$ . There are three stable forms of oxygen:  $^{16}\text{O}$ ,  $^{17}\text{O}$ , and  $^{18}\text{O}$ . The lightest one, is the most abundant, while  $^{17}\text{O}$  and  $^{18}\text{O}$  are less common in nature.

There are nine different stable water configurations, the most common of which are  $^1\text{H}^1\text{H}^{16}\text{O}$ ,  $^1\text{H}^2\text{H}^{16}\text{O}$ , and  $^1\text{H}^1\text{H}^{18}\text{O}$ . The masses of various stable water configurations differ, as do their physical and chemical properties. These differences result in isotopic fractionation or changes in stable isotope abundances at the beginning and end of physical, chemical, or biological processes. Because of fractionation, stable isotopes are sometimes referred to as "fingerprints" used in determining the origin of water [20].

The stable isotope composition of water is represented by  $\delta^{18}\text{O}$  and  $\delta^2\text{H}$ , with  $\delta$ -value defined as the ratio of heavier to lighter isotope abundance in the sample ( $R_{\text{sample}}$ ) and the standard ( $R_{\text{standard}}$ ):  $\delta(\text{‰}) = R_{\text{sample}} / R_{\text{standard}} - 1$ . To express the stable isotope composition of water, the international VSMOW (Vienna Standard Mean Ocean Water) standard is used. Fresh water  $\delta$ -values are typically negative, indicating a decrease in  $^2\text{H}$  or/and  $^{18}\text{O}$  abundance compared to the standard.

Evaporation and condensation have a significant impact on the isotopic composition of water (Fig. 1). Water vapour is depleted in heavy isotopes when compared to the evaporating body. In contrast, rain contains more heavy isotopes than residual vapour. Air temperature has a strong influence on precipitation isotope content, resulting in higher  $\delta$ -values in the summer and lower  $\delta$ -values in the winter [11]. There is a linear correlation between  $^2\text{H}$  and  $^{18}\text{O}$  values in natural waters that are not affected by evaporation ( $\delta^2\text{H} = 8 \cdot \delta^{18}\text{O} + 10 \text{‰}$ ), known as a Global Meteoric Water Line (GMWL) [2]. The calculation of regression lines for local precipitation (Local Meteoric Water Line - LMWL) and ground water (Local Groundwater Line - LGWL) is a standard procedure in isotope hydrology. If there is no further evaporation, the isotopic composition of the precipitation usually remains unchanged once it enters the underground [11]. Nonetheless, mixing of different water masses causes changes in the stable isotope composition of groundwater [10].

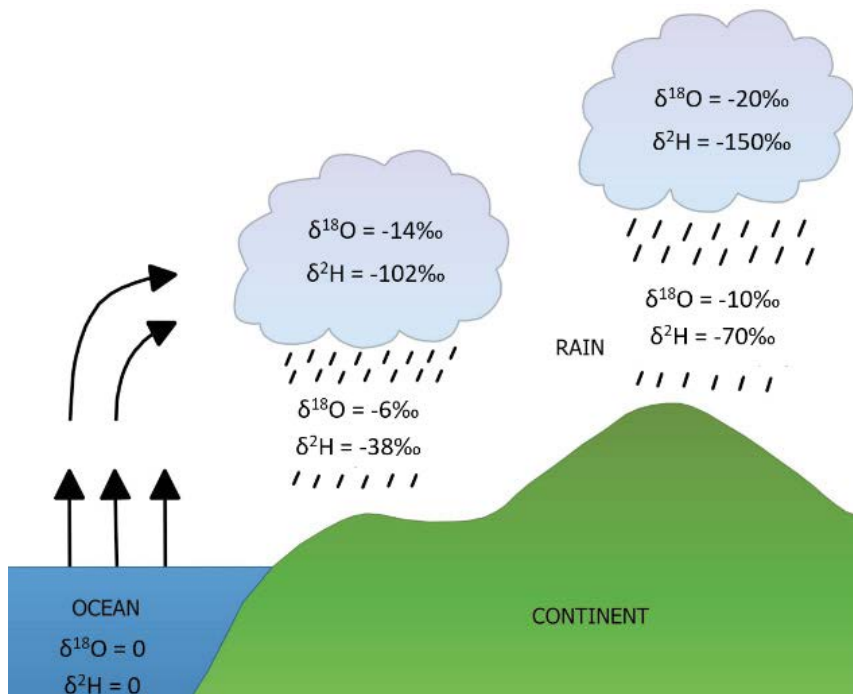


Figure 1 – The atmospheric part of water cycle and changes in stable isotope content caused by water evaporation and condensation.

In 1964, Dansgaard introduced the concept of d-excess, which is defined as follows:  $d\text{-excess} = \delta^2\text{H} - 8 \cdot \delta^{18}\text{O}$  [3]. D-excess values of around 10 ‰ indicate precipitation originating in the Atlantic Ocean, whereas values greater than 15 ‰ indicate precipitation originating in the Mediterranean [4].

The study area is the Bakar Bay spring discharge zone in western Croatia (Fig. 2).

For two years, weekly spring water samples were collected. We used a set of precipitation isotope data from the Kukuljanovo (KUK), Škalnica (SKAL), and Platak (PLAT) rain gauging stations to compare the isotopic content of precipitation and groundwater (Fig. 2). Some of these data have already been used in hydrogeological analyses of the Rječina River catchment [7, 8]. To prevent evaporation, monthly totals were collected in 3.5-litre rain gauges containing 100 ml of paraffin oil. After being separated from the oil, the precipitation samples, same as groundwater samples, were stored in double-capped HDPE bottles. A Delta<sup>plus</sup>XP (Thermo Finnigan) isotope ratio mass spectrometer, with an HDOeq48/24 (IsoCal) equilibration unit and a Dual Inlet system (Thermo Finnigan) as peripherals, was used for the stable isotope measurements. For  $\delta^{18}\text{O}$ , measurement precision was better than 0.1 ‰, and for  $\delta^2\text{H}$ , it was better than 1 ‰.

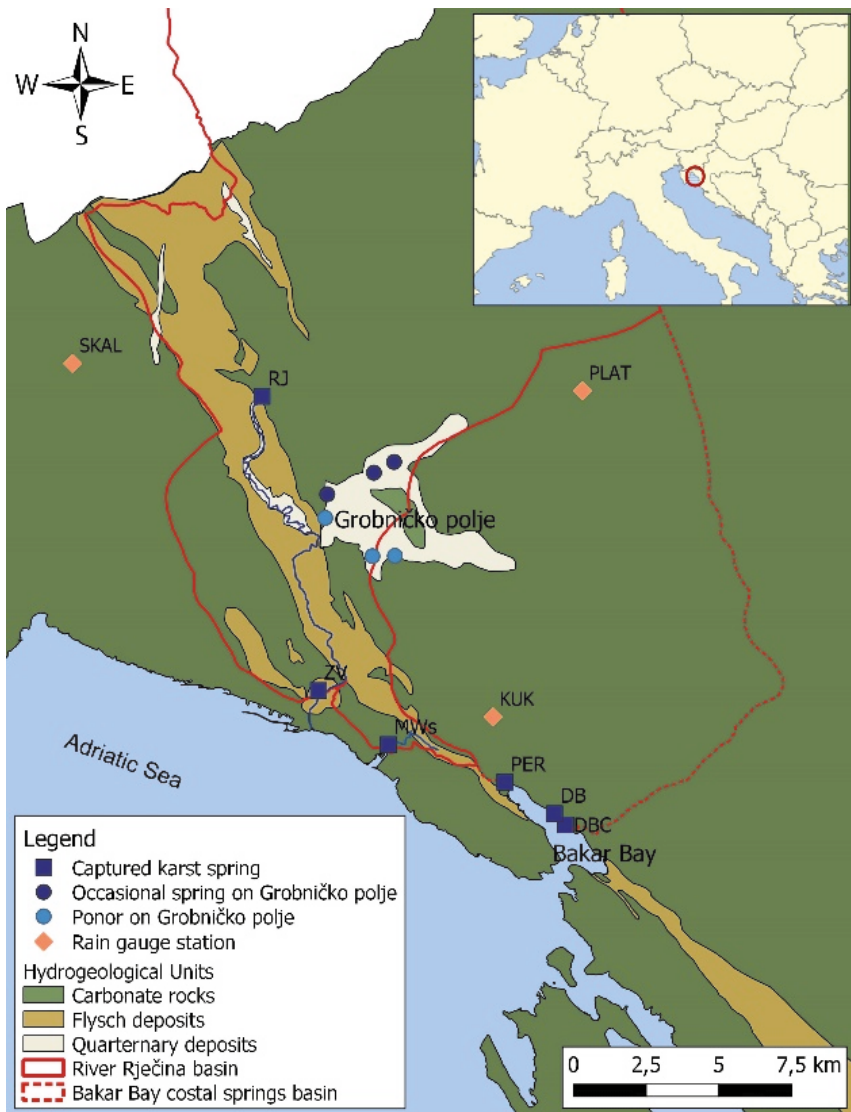


Figure 2 – The main map: a hydrogeological map of the study area showing basins of Rječina River and coastal springs in the Bakar Bay. The map also shows: the main karst springs (RJ – Rječina Spring, ZV – Zvir, MWs – Martinšćica wells, PER – Perilo, DB – Dobra, DBC – Dobrica), the Rječina River (blue line on the main map), and rain gauge stations for sampling cumulative monthly precipitation (KUK – Kukuljanovo, SKAL – Škalnica, PLAT – Platak). Upper right corner: the position of the study area in Europe.

To analyse the groundwater stable isotope series, we used univariate time series analysis methods such as autocorrelation function (ACF) and autoregressive integrated moving average modelling (ARIMA) [1]. We used graphical representations of ACF to draw a conclusions about aquifer's karstification and retention capabilities, as well as to select the appropriate ARIMA model. Prior to ARIMA, we used an additive component model ( $\delta = l + s + sc$ ) to test the groundwater stable isotope time series for trends and seasonal variations, where  $l$  is a linear trend component determined by linear regression,  $s$  is a seasonal component determined by periodic regression, and  $sc$  is a stochastic component. The results were interpreted using the 0.05 level of statistical significance.

## Results and Discussion

For the study area and period, LMWLs for the warm part of the hydrological year ( $\delta^2\text{H} = 8.05 \cdot \delta^{18}\text{O} + 8.52 \text{ ‰}$ ;  $R^2=0.89$ ) and cold part of the hydrological year ( $\delta^2\text{H} = 8.04 \cdot \delta^{18}\text{O} + 13.96 \text{ ‰}$ ;  $R^2=0.99$ ) were already presented in [7]. The division of the LMWL into summer and winter seasons was justified by previous studies. These have shown that the rainy season from October to April contributes more to groundwater recharge in the study area than the precipitation that falls during the summer season [7,8]. Figure 3 shows that the  $\delta$ -values of all three springs (PER, DB, and DBC) agree well with the LMWL for the cold season, indicating that the groundwater is primarily fed by winter precipitation. LGWL for PER, DB, and DBC, as shown in Fig. 3 ( $\delta^2\text{H} = 8.37 \cdot \delta^{18}\text{O} + 17.6 \text{ ‰}$ ;  $R^2=0.95$ ), further supports this conclusion.

Figure 4 shows large variations in the d-excess for rainwater: values in the winter months are significantly higher than values in the summer months of the hydrologic year. Since precipitation is generally lower in the summer months than in the winter months, a weighted average of d-excess was calculated: KUK (12.9 ‰), SKAL (14.71 ‰) and PLAT (14.66 ‰) [7]. Values for SKAL and PLAT correspond to the average values of groundwater d-excess for DBC ( $14.67 \pm 0.73$ ) ‰, DB ( $14.82 \pm 0.73$ ) ‰, and PER ( $14.53 \pm 0.73$ ) ‰.

Due to the strong and statistically significant correlation between  $\delta^{18}\text{O}$  and  $\delta^2\text{H}$  values ( $R=0.97$ ,  $p < 0.001$ ), only  $\delta^{18}\text{O}$  values were used for time series analysis. The ACF of the groundwater  $\delta^{18}\text{O}$  series was analyzed to obtain information about the system's karstification. Figure 5 shows the ACFs of the  $\delta^{18}\text{O}$  series for PER, DB, and DBC.

The shape of the ACF discharge graph is commonly used to determine the retention capacity and degree of karstification of the karst aquifer [17]. The karst system's "memory effect" is the time required for auto-correlation coefficients  $r(k)_{xx}$  to fall below 0.2 [9]. We used the same reasoning to interpret  $\delta^{18}\text{O}$  ACFs (Fig. 5). The ACFs do not decrease continuously but exhibit two types of decline, supporting the interpretation of the aquifers' dual nature. Initially, all three ACFs drop rapidly with steep slopes. The gradients begin to decline after five weeks. The ACF for PER decreases more rapidly, and its autocorrelation factors become statistically insignificant after eight weeks; whereas the ACFs for DB and DBC decrease more gradually, and their autocorrelation factors remain statistically significant for eleven weeks. The slower declines in DB and DBC ACFs suggest that DB and DBC have a greater ability to retain water than PER. This could also indicate a more developed karst channel system in the case of PER versus DB and DBC.

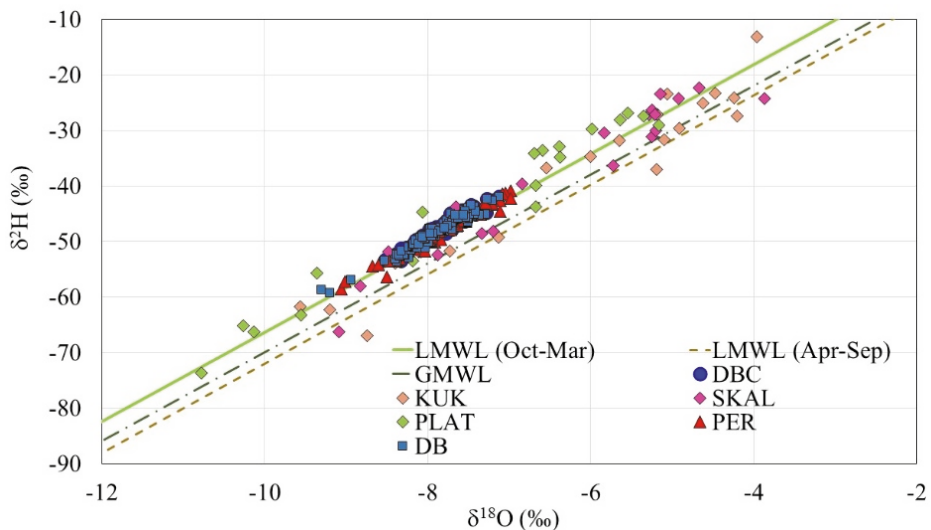


Figure 3 – Correlation diagram of  $\delta^2\text{H}$  and  $\delta^{18}\text{O}$  values for precipitation collected at Kukuljanovo (KUK), Škalnica (SKAL), and Platak (PLAT) stations, as well as groundwater collected at Dobrica (DBC), Dobra (DB) and Perilo (PER). Local meteoric water lines (LMWLs) for precipitation in the warm and cold seasons of the hydrological year, as well as a global meteoric water line (GMWL) are also presented.

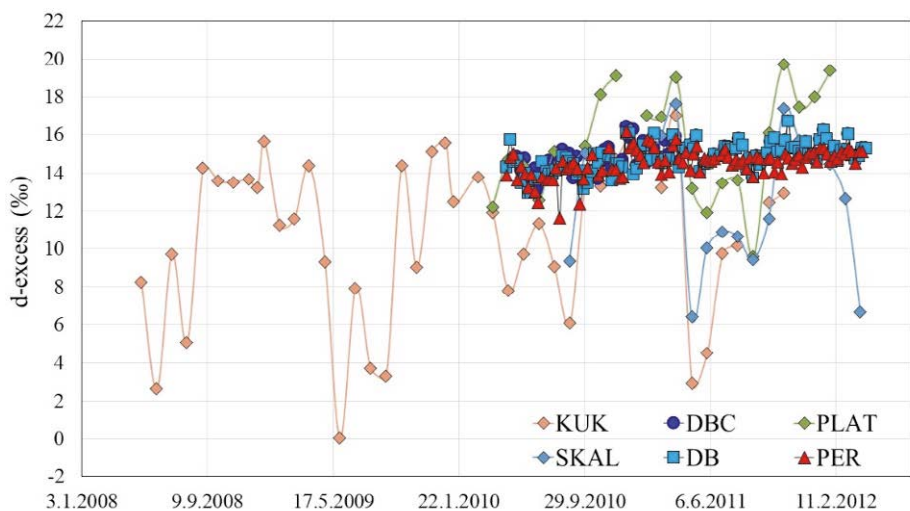


Figure 4 – D-excess values for precipitation collected at the stations Kukuljanovo (KUK), Škalnica (SKAL), and Platak (PLAT), and spring water from Dobrica (DBC), Dobra (DB) and Perilo (PER).

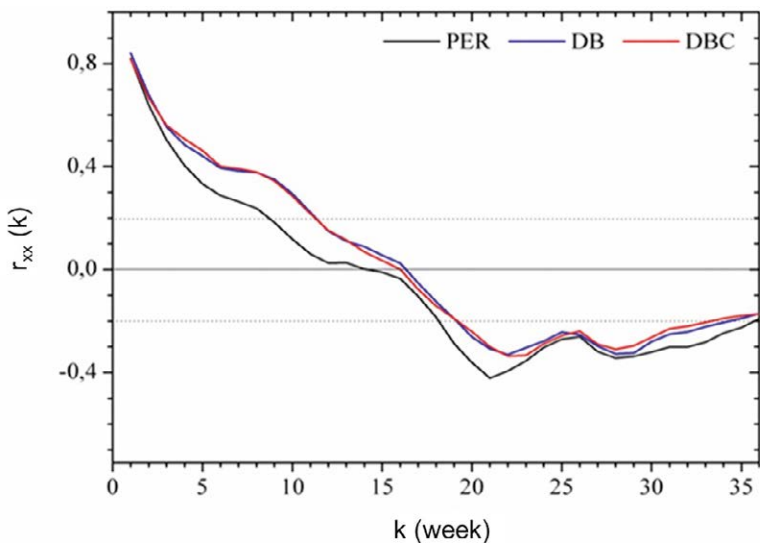


Figure 5 – Perilo (PER), Dobra (DB), and Dobrica (DBC) autocorrelation functions for  $\delta^{18}\text{O}$  time series.

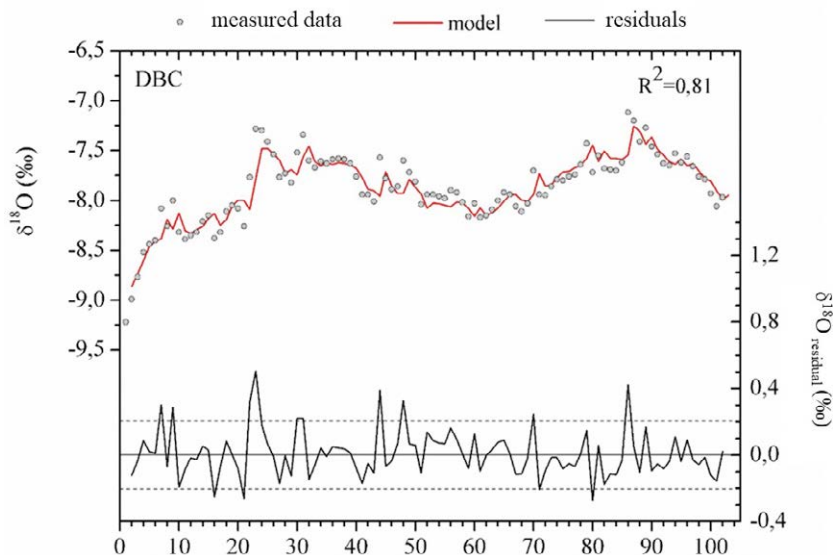


Figure 6 – Actual  $\delta^{18}\text{O}$  data from Dobrica, fitted model (created with linear regression, periodic regression, and ARIMA (1,0,0)), and residuals. The circles in the upper part of the graph represent the measured data for  $\delta^{18}\text{O}$  in water. A red line represents the fitted model. Deviations from the fitted model are represented by a black solid line in the lower part of the graph.

Since ARIMA results for PER and DB have already been published [8], this paper includes only DBC results. Significant linear and seasonal trends were observed:  $\delta^{18}\text{O} = -8.07 + 0.004 \cdot t - 0.32 \cdot \cos((2\pi/52) \cdot t + 2.32)$  ( $R^2=0.65$ ), where  $t$  is a time period (a week). There were no seasonal changes in the  $\delta^{18}\text{O}$  values of the monthly precipitation samples observed during the study period [7,8]. As a result, we conclude that seasonality in groundwater  $\delta^{18}\text{O}$  time series is caused by aquifer characteristics such as rapid infiltration and discharge of heavy rain, as well as the predominance of winter precipitation in replenishing groundwater reserves. Indeed, the strongest  $\delta^{18}\text{O}$  shifts to higher values were observed during the cold part of the hydrological year at the time of the heaviest precipitation. This indicates that precipitation infiltrated rapidly into the subsurface and reached springs in a short time. In contrast, groundwater had the lowest delta values during the warm part of the hydrologic year and these were without significant fluctuations. There were no heavy rain events during this period and we can conclude that the water sampled at the springs during this period came from the aquifer water reserves. The low delta values indicate that snowmelt probably plays the most important role in recharging the aquifer. This situation suggests that the systems analyzed are best described by the so-called dual porosity model. Such a model includes a fissure porous part of the aquifer characterized by baseflow whose activity is most evident during dry seasons. The second part of the model consists of a developed network of karst channels that respond rapidly to intense precipitation events.

ARIMA modeling of the  $\delta^{18}\text{O}$  series was performed after seasonal and linear trends were removed from the series and stationarity of the residual series was achieved. AR (1) (i.e., ARIMA (1,0,0) model) proved to be the best model for all three springs. The actual data, fitted data, and  $\delta^{18}\text{O}$  DBC residuals are shown in Fig. 6. The largest deviation from the statistical models was found for samples collected during heavy rainfall. For PER they were up to 1.2 ‰, while for DB and DBC they were not higher than 0.5 ‰. This difference in residuals could be explained by the greater karstification of the hinterland of PER compared to DB and DBC. The good agreement of measured and modelled values ( $R^2 = 0.81$ ) obtained by ARIMA (Fig. 6), also supports the idea of the DBC hinterland having a lower karstification degree and higher retention capability than PER ( $R^2 = 0.76$ ).

## Conclusions

To protect drinking water sources and use them sustainably, we need to understand how aquifers work. Karst aquifers are well-known for their complexity and research difficulty. Scientists have long agreed that multidisciplinary research is essential, and isotopic hydrology is an excellent example of multidisciplinary karst aquifer research.

This paper presents the findings of a two-year sampling at three karst springs in Bakar Bay (Croatia), as well as rain gauge stations in their vicinity. Based on the isotopic composition of the collected samples, we concluded that these karst springs are primarily fed by winter precipitation. Temporal changes in groundwater isotopic composition show a seasonal pattern not seen in precipitation. As a consequence, the seasonal oscillation of isotopic composition is interpreted as a function of the karst system itself, i.e. as a dual porosity model consisting of a fissure-porous aquifer (characterized by baseflow during the dry season) and highly developed karstic channels (characterized by rapid infiltration and strong discharge during heavy rainfall). The analysis of auto-correlation functions and time



series show that there is a difference in the degree of karstification of individual springs, with a higher degree of karstification indicating a greater sensitivity to potential pollution.

## Funding

This work was supported by the University of Rijeka under the project numbers: uniri-pr-prirod-19-24, UNIRI CLASS – A1-21-8 34, uniri-technic-18-298 and uniri-drustv-18-284-1456.

## References

- [1] Box G. E., Jenkins G. M., Reinsel G. C. (2008) - *Time series analysis: forecasting and control*, 4th ed., John Wiley & Sons, New Jersey.
- [2] Craig, H. (1961) - *Isotopic Variations in Meteoric Waters*. Science, 133(3465), 1702–1703.
- [3] Dansgaard, W. (1964) - *Stable isotopes in precipitation*. Tellus 16, 436–468.
- [4] Gat J.R., Carmi I. (1987) - *Effect of climate changes on the precipitation patterns and isotopic composition of water in a climate transition zone: case of the Eastern Mediterranean Sea area*, In: IAHS Publ. No. 168, 513–524
- [5] Goldscheider N., Chen Z., Auler A.S., Bakalowicz M., Broda S., Drew D., Hartmann J., Jiang G., Moosdorf N., Stevanović Z., et al. (2020) - *Global distribution of carbonate rocks and karst water resources*. Hydrogeol. J. 28, 1661–1677.
- [6] Iacurto S., Grelle G., De Filippi F.M., Sappa G. (2021) - *Karst Recharge Areas Identified by Combined Application of Isotopes and Hydrogeological Budget*. Water, 13(14):1965.
- [7] Mance D., Radišić M., Lenac D., Rubinić J. (2022) - *Hydrological Behavior of Karst Systems Identified by Statistical Analyses of Stable Isotope Monitoring Results*. Hydrol. 9(5), 82.
- [8] Mance D., Hunajk T., Lenac D., Rubinić J., Roller-Lutz, Z. (2014) - *Stable isotope analysis of the karst hydrological systems in the Bay of Kvarner (Croatia)*. Appl. Radiat. Isot. 90, 23–34.
- [9] Mangin, A. (1984) - *Pour une meilleure connaissance des systèmes hydrologiques à partir des analyses corrélatoire et spectrale*. J. Hydrol. 67, 25–43.
- [10] McGuire K., McDonnell J.J. (2006) - *A review and evaluation of catchment transit time modelling*. J. Hydrol. 330, 543–563.
- [11] Mook, W.G. (ed.) (2001) - *Environmental Isotopes in the Hydrological Cycle: Principles and applications*, UNESCO/ IAEA, Paris.
- [12] Paar D., Mance D., Stroj A., Pavić M. (2019) - *Northern Velebit (Croatia) karst hydrological system: Results of a preliminary  $^2\text{H}$  and  $^{18}\text{O}$  stable isotope study*. Geol. Croat. 72(3), 205–213.
- [13] Palcsu L., Gessert A., Túri M., Kovács A., Futó I., Orsovszki J., Puskás-Preszner A., Temovski M., Koltai G. (2021) - *Long-term time series of environmental tracers reveal recharge and discharge conditions in shallow karst aquifers in Hungary and Slovakia*, J. Hydrol. Reg. Stud. 100858 (36).

- [14] Radišić M, Rubinić J, Ružić I, Brozinčević A. (2021) - *Hydrological System of the Plitvice Lakes—Trends and Changes in Water Levels, Inflows, and Losses*. Hydrol. 174(8).
- [15] Rusjan S., Sapač K., Petrič M., Lojen S., Bezak N. (2019) - *Identifying the hydrological behavior of a complex karst system using stable isotopes*. J. Hydrol. 577, 123956.
- [16] Sappa G., Vitale S., Ferranti F. (2018) - *Identifying Karst Aquifer Recharge Areas using Environmental Isotopes: A Case Study in Central Italy*. Geosciences, 351(8).
- [17] Sivelle V., Jourde, H. (2021) - *A methodology for the assessment of groundwater resource variability in karst catchments with sparse temporal measurements*. Hydrogeol J 29, 137–157.
- [18] Stevanović, Z. (2019) - *Karst waters in potable water supply: A global scale overview*. Environ. Earth Sci., 662(78).
- [19] Stroj A., Briški M., Oštrić M. (2020) - *Study of Groundwater Flow Properties in a Karst System by Coupled Analysis of Diverse Environmental Tracers and Discharge Dynamics*. Water, 12(9):2442.
- [20] Tweed S., Leblanc M., Cartwright I., Bass A., Travi Y., Marc V., Nguyen Bach T., Dang Duc N., Massuel S., Saravana Kumar U. (2019) - *Stable Isotopes of Water in Hydrogeology*, Encyclopedia of Water, doi: 10.1002/9781119300762.wsts0154.